ISBN: 978-3-95450-212-7 ISSN: 2673-5482 doi:10.18429/JACoW-CYCLOTRONS2022-WEPO002

A COMPARSION STUDY OF THE DESIGNING MODELS OF RANGE MODULATOR BY USING FLUKA SIMULATION CODES*

Yue Wang, Li Sui†, Yihao Gong, Jiancheng Liu, Qiaojuan Wang
China Institute of Atomic Energy, Beijing, China
National Innovation Center of Radiation Application, Beijing, China

Abstract

In this study, we investigated the optimization of the range modulator. Range modulator used in proton radiotherapy is expected to be accurate enough to achieve spread-out Bragg peak (SOBP). Based on the theory of Thomas Bortfeld, four different range modulator models were designed and compared using FLUKA simulation codes. The four models were: uneven ridge filter, smooth ridge filter, uneven range modulator wheel, and smooth range modulator wheel. Using 100 MeV and 230 MeV proton beams, the dose spatial distribution of the four models were calculated when the SOBP sections were 3, 5, 10, and 20 cm. The results showed that in ideal motion condition, the four models all showed the ideal range modulation effect. The best average value of the difference was less than 2%, while the worst one was still less than 5%. The evenness of the smooth models is improved compared with the uneven models. The smooth ridge filter model performed best. Based on this model, we tried to realize the movement of the SOBP region by adding a binary shielding layer. The results showed that the SOBP region can move in a small range at the expense of acceptable accuracy error. This study provides a design reference for the range modulator in proton therapy, and provides a new technical scheme to fill the target area for precise therapy.

INTRODUCTION

Radiation therapy is one of the three most effective treatments for cancer, the other two being chemotherapy and surgical resection. Radiation therapy refers to the use of radiation to irradiate the tumor area, and the relative biological effect of the radiation to damage the DNA of malignant tumor cells, so as to achieve the purpose of killing or reducing cancer cells.

Charged particle therapy (CPT), including proton and heavy ion therapy, is currently the advanced direction of radiotherapy. The advantage of CPT is that the concentrated dose distribution pattern of charged particles makes it possible to artificially and accurately control the dose distribution in the target area, thereby achieving higher tumor control probability and lower normal tissue complication probability. The unique Bragg peak dose distribution pattern of protons and heavy ions makes the advantages of CPT possible [1]. Taking protons as an example, single-energy protons have a low dose before the human body, slowly increase the dose after entering the human body, climb rapidly to the terminal peak, and finally decline rapidly, achieving a high concentration of doses, of which the highest point of the dose is called Bragg peak [2], see Fig. 1. In actual use, Bragg peak needs to include the lesion to ensure an even and flat dose distribution in the target area. The Bragg peak of a single-energy proton ray is extremely narrow, generally between a few millimeters and one centimeter. It is impossible to encompass the lesion completely, so the Bragg peak needs to be widened. The most basic broadening way is to use particle beams of different energies to irradiate together, and superimpose them according to different weights to form a relatively gentle flat area in the target area [3]. In actual use, only one single energy particle beam can be provided at one time, so the device that can convert a single energy particle beam into a multi-energy particle beam with a specified weight ratio is needed, which is called range modulator. The range modulator to achieve SOBP is an extremely important part of the treatment head system of CPT equipment.

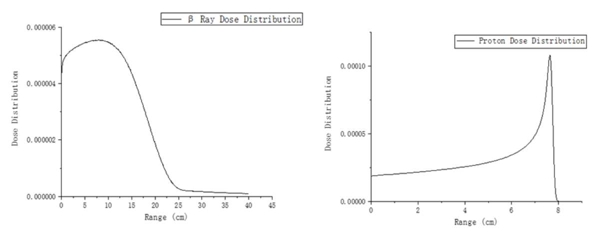

Figure 1: The dose distribution of β-ray and proton.

The Bragg peak of the single energy particle beam is broadened to a flat dose distribution region by the modulator's geometry and relative motion. Because the parameters of the range modulator vary with different width and depth of certain SOBP, it is necessary to customize the range modulator according to the patient's situation in actual use, so it is of great significance to study the design process and optimization of the range modulator.

SIMULATION METHOD

Since experimental opportunities are precious, it is necessary to conduct simulation studies of range modulators prior to experiments.

Monte Carlo Simulation Codes

In this study, FLUKA was selected as the Monte Carlo (MC) simulation software. FLUKA is a universal MC particle transport simulation software that runs on Linux. Through continuous updates, FLKUA now supports the transport process and measurement simulation of about 60 kinds of particles including photons, electrons, protons, and various heavy ions in magnetic field, electric field, and thermal field, and supports users to program the particle

* Work supported by CIAE Youth Fund YC202212000201
† lisui@ciae.ac.cn

distribution and motion in the transport process through the FORTRAN interface to realize complex processes. Through custom program compilation, FLUKA allows users to perform partial or global spatial calculations during particle transport. FLUKA itself is difficult to build complex geometric structures, and users can build complex geometry through CG tool kits or SimpleGeo.

Typical Range Modulator Models

The existing commonly used range modulators are divided into range modulator wheels (RMW) and ridge filters (RF). Through periodic movement, the fixed particle beam passes through the shielding layer of different thickness. The particle energy is the smallest when passing through the thickest area, while the particle energy is the largest when passing through the smallest thickness area. The area of different thicknesses and the particle movement speed are adjusted to achieve the distribution of scanning time in line with the weight ratio, thereby realizing the SOBP of the single-energy particle beam.

The common design method of the range modulator wheel is to divide the entire circumferential area into several equal pieces, each piece is divided according to the center angle of the multi-energy particle beam weight, and each small piece divided has a different specific material thickness (Fig. 2). RMW rotates at a uniform speed under the irradiation of the particle beam, and the size of the center angle determines the residence time of the particle beam in this area, and the corresponding material thickness determines the energy of the outgoing particle beam, so that the dose average is achieved on the time scale [4].

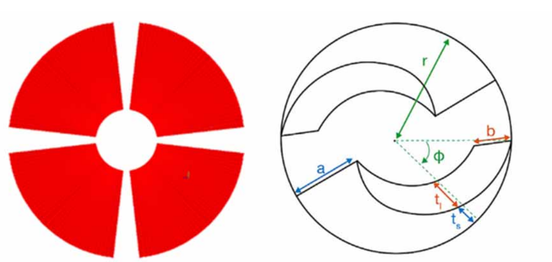

Figure 2: Typical range modulator wheel.

In addition to the range modulator wheel, another commonly used range modulator is the ridge filter. Ridge filters, also known as washboard filters, generally consist of continuous triangular pyramids. Each triangular pyramid section is generally not a rectilinear triangle in the strict sense, but a block of different thicknesses. The particle beam passes through the highest place with the lowest exit energy and the highest energy at the lowest, and the width of each block determines the distribution weight [5]. Generally, the size of the whole washboard is about 10 to 20 cm, and the mid-ridge filter is used to move laterally, and the particle beam skims over the surface of the ridge filter, and is broadened by energy-reducing materials of different thicknesses and widths.

Models and SOBP Simulation

Based on the theory of Thomas Bortfeld and simplified adaptation function method, four different range modulator models were designed and compared by using the FLUKA simulation codes. The four models were: uneven ridge filter, smooth ridge filter, uneven range modulator wheel, and smooth range modulator wheel.

Taking ridge filter modelling as an example, a single ridge tooth was modelled first, and the overall effect can be achieved by motion equivalence. From the size conversion, one single ridged tooth was divided into a PMMA cuboid combination with a thickness of 73 layers, and a 73-layer cuboid was constructed in the void area, with the Z coordinate of each layer set to the PMMA thickness, the Y coordinate set to the weight adaptation width, and the X coordinate is uniformly set to 2 cm to build a uniform "triangular pyramid", while a gap of 1e-6 cm inserted between each layer. The material used to fill these voids is vacuum, so there is no additional energy loss. The OR operation in the Boolean operation was used to combine the above spatial volumes into a whole, and the material was selected as PMMA to obtain a single ridged tooth structure of the ridge filter, see Fig. 3. The smoothing filter model was obtained by converting its edges into elliptic curves by quadratic term fitting. The range modulation wheel model construction methods were similar.

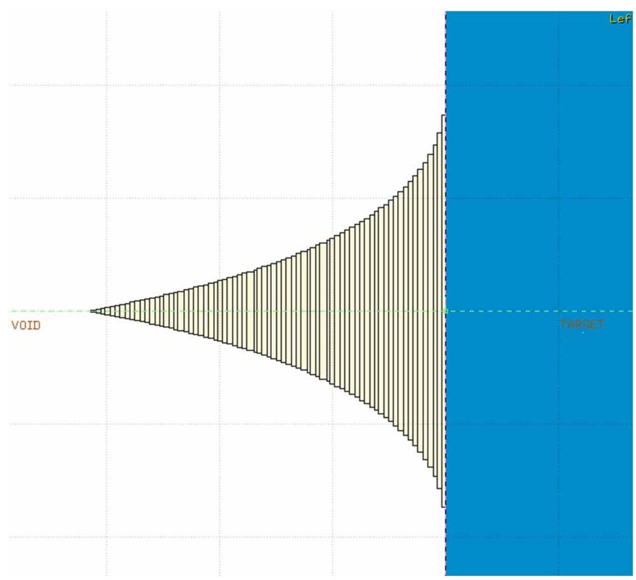

Figure 3: A single ridge filter tooth structure.

RESULTS

By adjusting the sensitivity coefficient k value in the adaptation function method, the proton Bragg peak broadening curve gradually changed from a downward trend to an uptrend, and the best broadening effect existed. According to the calculation of flatness and flat width, the best broadening effect was achieved for the ridge filter and the range modulation wheel under the corresponding weigh ratio

ISBN: 978-3-95450-212-7 ISSN: 2673-5482 doi:10.18429/JACoW-CYCLOTRONS2022-WEPO002

Table 1: SOBP Effects of the Four Models

Average Value of the Difference	Uneven Ridge Filter	Smooth Ridge Filter	Uneven Range Modulator Wheel	Smooth Range Modulator Wheel
100 MeV - 3 cm SOBP	0.99%	0.86%	0.92%	0.88%
100 MeV - 5 cm SOBP	1.18%	1.02%	1.10%	1.06%
230 MeV - 10 cm SOBP	1.21%	0.94%	1.24%	0.96%
230 MeV - 20 cm SOBP	1.62%	1.08%	1.52%	1.06%

when k = 0.7. At the 98% confidence level, the widening results of the uneven ridge filter were as follows: the SOBP ping area was [4.10, 7.42] cm, and the flatness of the corresponding flat area was 99.14%. The remaining results can be found in Table 1.

The results showed that in ideal motion condition, the four models all showed the ideal range modulation effect. The average value of the difference was less than 2%. The evenness of the smooth models is improved compared with the uneven models. The smooth ridge filter model performed best.

DISCUSSION

For a certain sensitivity coefficient k, the broadening results of the range modulator designed according to the corresponding weights had an upward slope trend compared with the multi-energy particle weight matching model, which indicates that the high-energy region weight of the physical model was higher than that of the theoretical model.

The possible reason is that the construction of the physical model increased the scattering effect of the particles [6-8]. Because in the theoretical model, through the user-defined program, single-energy proton beams of different intensities and different energies were shot vertically into the water model target area. And the area passed through before entering the target area was vacuum, and there was no side scattering phenomenon, and side scattering can exist only when entering the water model. In the physical model, the equivalent single-energy proton beams first passed through the PMMA shielding layer of different thicknesses and then entered the water, which increased the process of proton movement in the PMMA material. The protons in the scattering bifurcation part didn't pass through the expected length of the PMMA shield to attenuate enough energy, but kept the higher energy out of the material through the vacuum and hit the target, leading to the detector received additional high-energy proton signals. At the same time, the lower the energy, the coarser the trail, and the expected share of low-energy protons through the shielding layer was larger, and the share of lateral scattering was larger. The higher the energy, the finer the trail, the smaller the bifurcation, the thinner the shield that was expected to pass through, and the smaller the chance of lateral scattering. On the whole, the physical model had an extra share of side scatter, and it was expected that low-energy protons were more likely to be side-scattered to reduce energy attenuation, thereby increasing the share of high-energy regions.

In order to verify whether the weight ratio changed due to the dose contribution of secondary particles, the two physical models of k = 0.7 and k = 2.1 were divided into fine grids in the YZ direction to simulate the dose distribution. The upper result in Fig. 4 is the YZ direction dose distribution at k = 0.7, it can be seen that protons were uniformly deposited at this scale, basically no obvious deviation, although more energy is deposited in the range modulator, and the proton dose injected into the water mold was low overall, but it is relatively uniform and the broadening effect is the best. Another result is the YZ plane dose distribution while k = 2.1, showing an obvious discrete state. The energy deposition is concentrated around Y = 0 and Z = 0, and the thickness of the PMMA layer passed through by the proton beam near the Y = 0 straight line corresponded to the smaller the energy injected into the water mode, and the more shares of these protons were deposited in the modulator. And the proportion of protons after injection into water naturally decreased. However, the proton beam deviating from Y = 0 was less deposited in the modulator, and the proportion of injection into the water mold values from k = 0.7 and k = 2.1 can also be verified from naturally increased, so the effect of widening the flat area

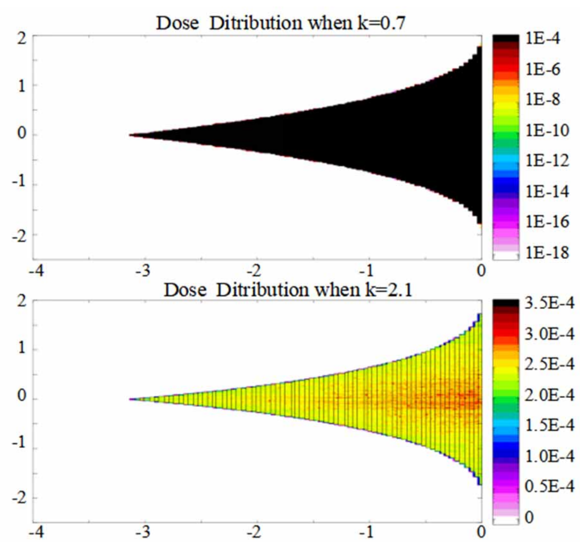

Figure 4: Dose distribution of two physical models of k = 0.7 (top) and k = 2.1 (bottom).

ISBN: 978-3-95450-212-7 ISSN: 2673-5482 doi:10.18429/JACoW-CYCLOTRONS2022-WEPO002

was tilted upward. The un-normalized water mode dose the side of the two models: the dose in the broadened ping area when k = 0.7 was 3.38E-5, while the dose in the k = 2.1 broadened flat area fluctuated from 3.3E-5 to 3.70E-5, which showed that there was a difference in dose deposition in the physical model of k = 2.1, and less dose was deposited compared with the k = 0.7 model.

POTENTIAL OPTIMIZATION

On the basis of smooth RF model, we tried to realize the movement of the SOBP region by adding a binary shielding layer. The results showed that the SOBP region can move in a small range at the expense of acceptable accuracy error.

CONCLUSION

The essence of proton range modulation is to weight protons of different energies. In this study, FLUKA was used for Monte Carlo calculation, and the broadening results of four different range modulator models were calculated and compared, and finally the optimal broadening model was obtained by screening. Based on the calculation results, the influence of secondary particle dose contribution in the range modulation process was discussed, and possible improvement schemes were explored to lay a foundation for subsequent research.

ACKNOWLEDGEMENTS

Valuable discussions and help from Dr. J. L. Wang of CIAE are acknowledged.

REFERENCES

[1] S. Michiels *et al.*, "Patient-specific bolus for range shifter air gap reduction in intensity-modulated proton therapy of head-and-neck cancer studied with Monte Carlo based plan optimization", *Radiotherapy and Oncology*, vol. 128, no. 1, pp. 161-166, 2018. doi:10.1016/j.radonc.2017.09.006

[2] H. Suit *et al.*, "Proton vs carbon ion beams in the definitive radiation treatment of cancer patients", *Radiotherapy and Oncology*, vol. 95, no. 1, pp. 3-22, 2010. doi:10.1016/j.radonc.2010.01.015

[3] C. H. Kim *et al.*, "Practical biological spread-out Bragg peak design for a carbon beam", *J. Korean Phys. Soc.*, vol. 67, pp. 1440-1443, 2015. doi:10.3938/jkps.67.1440

[4] S. B. Jia *et al.*, "Designing a range modulator wheel to spread-out the Bragg peak for a passive proton therapy facility", *Nucl. Instrum. Methods Phys. Res., Sect. A*, vol. 806, pp. 101-108, 2016. doi:10.1016/j.nima.2015.10.006

[5] M. H. Jung *et al.*, "Design of a ridge filter for spread-out Bragg-peak production in a pulsed 100-MeV proton beam", *J. Korean Phys. Soc.*, vol. 63, pp. 1441-1445, 2013. doi:10.3938/jkps.63.1441

[6] L. Rezaee, "Design of spread-out Bragg peaks in hadron therapy with oxygen ions", *Reports of Practical Oncology & Radiotherapy*, vol. 23, no. 5, pp. 433-441, 2018. doi:10.1016/j.rpor.2018.08.004

[7] I. Park, "A new approach to produce spread-out Bragg peak using the MINUIT fit", *Curr. Appl Phys.*, vol. 9, no. 4, pp. 852-855, 2009. doi:10.1016/j.cap.2008.07.022

[8] D. W. Kim *et al.*, "Prediction of output factor, range, and spread-out Bragg peak for proton therapy", *Med. Dosim.*, vol. 36, no. 2, pp. 145-152, 2011. doi:10.1016/j.meddos.2010.02.006